JOURNAL OF AIRCRAFT
Vol. 41, No. 5, September–October 2004

Limit-Cycle Oscillations of a Typical Airfoil in Transonic Flow

Denis B. Kholodar*
U.S. Air Force Academy, Colorado Springs, Colorado 80840
and
Earl H. Dowell,† Jeffrey P. Thomas,‡ and Kenneth C. Hall§
Duke University, Durham, North Carolina 27708

Using an inviscid flow computational-fluid-dynamic model and a harmonic balance flow solver, a parametric investigation of how structural-inertial parameters and freestream Mach number of a transonic flow affect the limit-cycle oscillation characteristics of a typical two-degree-of-freedom transonic airfoil configuration is presented. The computational efficiency of the harmonic balance aerodynamic model allows a much more thorough exploration of the parameter range than has been possible previously.

Nomenclature

a	=	nondimensional location of airfoil elastic axis, $a = e/b$
b, c	=	semichord and chord, respectively
$\bar{c}_l, \bar{c}_m$	=	nondimensional coefficients of lift and moment about elastic axis for simple harmonic motion
e	=	location of airfoil elastic axis, measured positive aft of airfoil midchord
$h, \bar{h}$	=	airfoil plunge degree of freedom and its nondimensional amplitude, respectively; $\bar{h}$ is identical to h/b
I_α	=	second moment of inertia about elastic axis
L	=	aerodynamic lift
K_h, K_α	=	airfoil plunge stiffness and torsional stiffness about elastic axis, respectively
M	=	freestream Mach number
$M_{\text{e.a.}}$	=	aerodynamic moment about elastic axis
m	=	airfoil sectional mass
r_α	=	radius of gyration of airfoil about elastic axis, r_α^2 is identical to I_α/mb^2
S_α	=	first moment of inertia about elastic axis or static unbalance
U	=	freestream velocity
V	=	reduced velocity; V is identical to $U/\omega_\alpha b$
x_α	=	airfoil static unbalance, x_α is identical to S_α/mb
$\alpha, \bar{\alpha}$	=	airfoil pitch degree of freedom and its nondimensional amplitude, respectively
μ	=	mass ratio; μ is identical to $m/\pi\rho b^2$
$\omega, \bar{\omega}$	=	frequency and reduced frequency based on airfoil chord, $\bar{\omega}$ is identical to $\omega c/U$
ω_α, ω_h	=	uncoupled natural frequencies of pitch and plunge degrees of freedom
ω_1, ω_2	=	coupled structural natural frequencies

Received 29 January 2003; revision received 9 August 2003; accepted for publication 31 August 2003.

*Research Associate, Department of Aeronautics. Previously Research Associate, Department of Mechanical Engineering, Duke University. Member AIAA.

†J. A. Jones Professor, Department of Mechanical Engineering and Materials Science, Director, Center for Nonlinear and Complex Systems, and Dean Emeritus, School of Engineering. Fellow AIAA.

‡Research Assistant Professor, Department of Mechanical Engineering and Materials Science. Member AIAA.

§Professor and Chairman, Department of Mechanical Engineering and Materials Science. Associate Fellow AIAA.

Introduction

TRANSONIC flow flutter and limit-cycle oscillations (LCO) are of significant interest in wing and aircraft design. The large expense incurred in both time- and frequency-domain transonic aerodynamic computations is the principal obstacle to the aeroelastician in obtaining a deeper understanding of these phenomena through a systematic parameter study.

In the past few years at Duke University, a number of computational-fluid-dynamic (CFD)-based time (dynamically) linearized codes have been developed and converted to the frequency domain. Recently, a novel nonlinear harmonic-balance (HB) solution method that extends the frequency-domain CFD models to the fully dynamically nonlinear range has been developed.[1] This method enables one to model efficiently nonlinear unsteady aerodynamic behavior corresponding to finite amplitude structural motion of a prescribed frequency and which can be subsequently used for modeling LCO behavior.[2] It is believed that HB-based LCO modeling will significantly advance the aeroelastician's capability to do rapid parametric studies.

Using a dynamically linearized option of the Euler HB model, the flutter boundary of a typical two-degree-of-freedom (DOF) airfoil aeroelastic configuration was determined (see Refs. 3 and 4). In the current work a subsequent LCO study of the same model undergoing large motions is described.

Governing Equations and Computational Method

Consider a typical two-DOF airfoil section with the equations of motion:

$$m\ddot{h} + S_\alpha\ddot{\alpha} + K_h h = -L, \qquad S_\alpha\ddot{h} + I_\alpha\ddot{\alpha} + K_\alpha\alpha = M_{\text{e.a.}} \tag{1}$$

Here the left-hand side terms represent a linear structural model for the plunge-and-pitch coordinates. The right-hand-side terms represent the aerodynamic loading terms, which for this study are based upon the harmonic balance solution approach applied to a CFD model of the inviscid Euler equations. A summary of the method, its application to parametric flutter analysis, and a CFD grid-convergence study are given in a recent work of the authors.[3]

For a more detailed description of the inviscid computational-fluid-dynamic harmonic-balance aerodynamic Euler-based method, see Ref. 5.

Rewriting the nonlinear aeroelastic equations in the frequency domain in terms of nondimensional variables yields

$$\left[-\bar{\omega}^2\begin{pmatrix}1 & x_\alpha\\ x_\alpha & r_\alpha^2\end{pmatrix} + \frac{4}{V^2}\begin{pmatrix}\omega_h^2/\omega_\alpha^2 & 0\\ 0 & r_\alpha^2\end{pmatrix}\right]\begin{Bmatrix}\bar{h}\\ \bar{\alpha}\end{Bmatrix} = \frac{4}{\pi\mu}\begin{Bmatrix}-\bar{c}_l(\bar{h},\bar{\alpha},\bar{\omega})\\ 2\bar{c}_m(\bar{h},\bar{\alpha},\bar{\omega})\end{Bmatrix} \tag{2}$$

Modeling LCO Behavior

Specifying a real valued amplitude of the pitch DOF as the independent variable $\bar{\alpha}$, the real and imaginary parts of Eq. (2) then constitute a system of four nonlinear real equations for the vector of unknowns:

$$\boldsymbol{L} = \begin{Bmatrix} \bar{\omega} \\ V \\ \left(\dfrac{\bar{h}}{\bar{\alpha}}\right)_{\mathrm{Re}} \\ \left(\dfrac{\bar{h}}{\bar{\alpha}}\right)_{\mathrm{Im}} \end{Bmatrix} \tag{3}$$

Equation (2) can then be written in the vector form $\boldsymbol{R}(\boldsymbol{L}) = \boldsymbol{0}$, or

$$\begin{Bmatrix} -\bar{\omega}^2\left(\dfrac{\bar{h}_r}{\bar{\alpha}}\right)_{\mathrm{Re}} & +\dfrac{4}{V^2}\dfrac{\omega_h^2}{\omega_\alpha^2}\left(\dfrac{\bar{h}}{\bar{\alpha}}\right)_{\mathrm{Re}} & -\bar{\omega}^2 x_\alpha & +\dfrac{4}{\pi\mu\bar{\alpha}}(\bar{c}_l)_{\mathrm{Re}} \\ -\bar{\omega}^2\left(\dfrac{\bar{h}}{\bar{\alpha}}\right)_{\mathrm{Im}} & +\dfrac{4}{V^2}\dfrac{\omega_h^2}{\omega_\alpha^2}\left(\dfrac{\bar{h}}{\bar{\alpha}}\right)_{\mathrm{Im}} & & +\dfrac{4}{\pi\mu\bar{\alpha}}(\bar{c}_l)_{\mathrm{Im}} \\ -\bar{\omega}^2 x_\alpha\left(\dfrac{\bar{h}}{\bar{\alpha}}\right)_{\mathrm{Re}} & -\bar{\omega}^2 r_\alpha^2 & +\dfrac{4}{V^2}r_\alpha^2 & -\dfrac{8}{\pi\mu\bar{\alpha}}(\bar{c}_m)_{\mathrm{Re}} \\ -\bar{\omega}^2 x_\alpha\left(\dfrac{\bar{h}}{\bar{\alpha}}\right)_{\mathrm{Im}} & & & -\dfrac{8}{\pi\mu\bar{\alpha}}(\bar{c}_m)_{\mathrm{Im}} \end{Bmatrix} = \boldsymbol{0} \tag{4}$$

As demonstrated in Ref. 2, a Newton–Raphson method was used to solve the system, Eq. (4).

$$\boldsymbol{L}^{n+1} = \boldsymbol{L}^n - \left[\frac{\partial \boldsymbol{R}(\boldsymbol{L}^n)}{\partial \boldsymbol{L}}\right]^{-1} \boldsymbol{R}(\boldsymbol{L}^n) \tag{5}$$

where the Jacobian matrix $\partial \boldsymbol{R}(\boldsymbol{L}_n)/\partial \boldsymbol{L}$ can be approximated using forward differences. For example,

$$\left.\frac{\partial \boldsymbol{R}(\boldsymbol{L}^n)}{\partial \boldsymbol{L}}\right|_{1,1} \equiv \frac{\partial \boldsymbol{R}_1(\boldsymbol{L}^n)}{\partial \bar{\omega}} \approx \frac{\boldsymbol{R}_1(\boldsymbol{L}^n, \bar{\omega}^n + \epsilon) - \boldsymbol{R}_1(\boldsymbol{L}^n, \bar{\omega}^n)}{\epsilon}$$

$$\left.\frac{\partial \boldsymbol{R}(\boldsymbol{L}^n)}{\partial \boldsymbol{L}}\right|_{1,2} \equiv \frac{\partial \boldsymbol{R}_1(\boldsymbol{L}^n)}{\partial V} \approx \frac{\boldsymbol{R}_1(\boldsymbol{L}^n, V^n + \epsilon) - \boldsymbol{R}_1(\boldsymbol{L}^n, V^n)}{\epsilon} \tag{6}$$

for a small ϵ. Thus, during each iteration the HB flow solver is run four times: one time to determine $\boldsymbol{R}$ for $\boldsymbol{L}^n$ and three more times to determine $\boldsymbol{R}$ for $\boldsymbol{L}^n$ with sensitivities in $\bar{\omega}$, $(\bar{h}/\bar{\alpha})_{\mathrm{Re}}$, and $(\bar{h}/\bar{\alpha})_{\mathrm{Im}}$. Once the values of Newton–Raphson's method sequence are sufficiently close to the root, the convergence is so rapid that only a few more values are needed.

Using the reduced flutter velocity, the frequency, and eigenvector obtained from a linearized aerodynamic model as starting solution, one can then calculate a LCO solution for a specified small amplitude of pitch $\bar{\alpha}$ in just a few iterations. The process can then be repeated for a larger LCO amplitude. Smaller amplitude increments must be used for successful convergence if the nonlinear effect is very strong.

One of the main objectives of this study is to determine the effects of aerodynamic nonlinearity of the flow on LCO behavior of the airfoil. The dependence of LCO behavior on the Mach number presents the greatest challenge especially for transonic Mach numbers.

In presenting the results, a distinction will be made with respect to stable LCO vs unstable LCO and weak vs strong (stable or unstable) LCO. To explain these terms, consider Fig. 1, which displays three generic curves for the amplitude of LCO vs reduced velocity. If the aerodynamic model is dynamically linear, then in this limiting case the LCO amplitude vs reduced velocity curve would simply be a vertical line indicating that the steady limit-cycle amplitude is infinite when the flutter boundary and the corresponding reduced velocity is reached and exceeded. Hence, a vertical or near-vertical

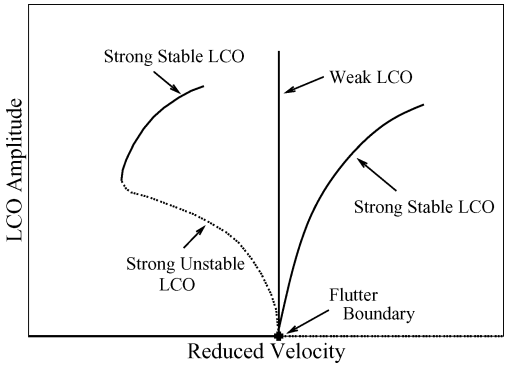

Fig. 1 Generic display of the LCO behavior.

graph of LCO amplitude vs reduced velocity is said to be a weak LCO. Note that a weak LCO in fact corresponds to a large LCO amplitude. Conversely if the LCO amplitude is smaller and the graph of LCO amplitude vs reduced velocity bends more to the right or left, it is said to be a strong LCO. Note that weak or strong refers to the strength of the (aerodynamic) nonlinearity, and the LCO amplitude itself is correspondingly large or small.

Now the other distinction to be emphasized is that between stable vs unstable LCO. If the LCO amplitude increases with increasing reduced velocity beyond the flutter boundary, then the LCO is said to be stable. Physically this means that LCO does not occur below the flutter boundary and that the LCO that occurs above the flutter boundary is stable with respect to small infinitesimal disturbances. Conversely, if the LCO amplitude increases as the reduced velocity decreases from the flutter boundary then the LCO is said to be unstable because LCO can now occur for reduced velocities below the flutter boundary. Moreover, a stability analysis for the LCO per se with respect to infinitesimal disturbances will usually show that any perturbation to this unstable LCO will lead to a transient motion that at large time will reach a new LCO that is stable (typically at a larger amplitude). Again see Fig. 1 for a generic display of this latter behavior. In the present work a perturbation stability analysis of the LCO per se has not been carried out, and the identification of stable or unstable LCO is made based solely on the dependence of LCO amplitude on reduced velocity as shown in Fig. 1.

The discussion of the LCO results begins with the dependence of LCO on mass and uncoupled natural frequencies ratios at Mach number $M = 0.8$.

LCO Sensitivity to Structural-Inertial Parameters

These LCO results are obtained for a NACA 64A010A airfoil with the following values of structural parameters: $x_\alpha = 0.25$, $r_\alpha^2 = 0.75$, and $a = -0.6$. These parameters match those of the previous flutter studies.[2] From these studies it is known that the solution variables (i.e., reduced velocity, frequency, and structural eigenmode) vary little with the mass ratio μ and flutter reduced velocities have a minimum near $\omega_h/\omega_\alpha \approx 1$. These same trends are also observed in the following LCO results (at a given LCO amplitude) for a Mach number of $M = 0.8$.

A distinct transition from stable LCO to weak LCO and then to unstable LCO as the ratio of uncoupled frequencies is increased is noted. In all cases a higher mass ratio is found to correspond to a higher reduced velocity (for a particular LCO amplitude) and a lower reduced frequency.

Also considered is harmonic convergence of the computed unsteady aerodynamic forces via the HB solver.

$$\omega_h/\omega_\alpha = 0.5$$

Figure 2a shows a stable LCO in terms of LCO amplitude vs reduced velocity. Employing just two harmonics in the HB solver provides a good level of harmonic convergence for moderate LCO amplitudes. The motion is plunge dominant at low amplitudes and becomes even more so ($|\bar{h}/\bar{\alpha}|$ increases) for large LCO amplitudes.

$$\omega_h/\omega_\alpha = 0.8, \qquad \omega_h/\omega_\alpha = 1.5$$

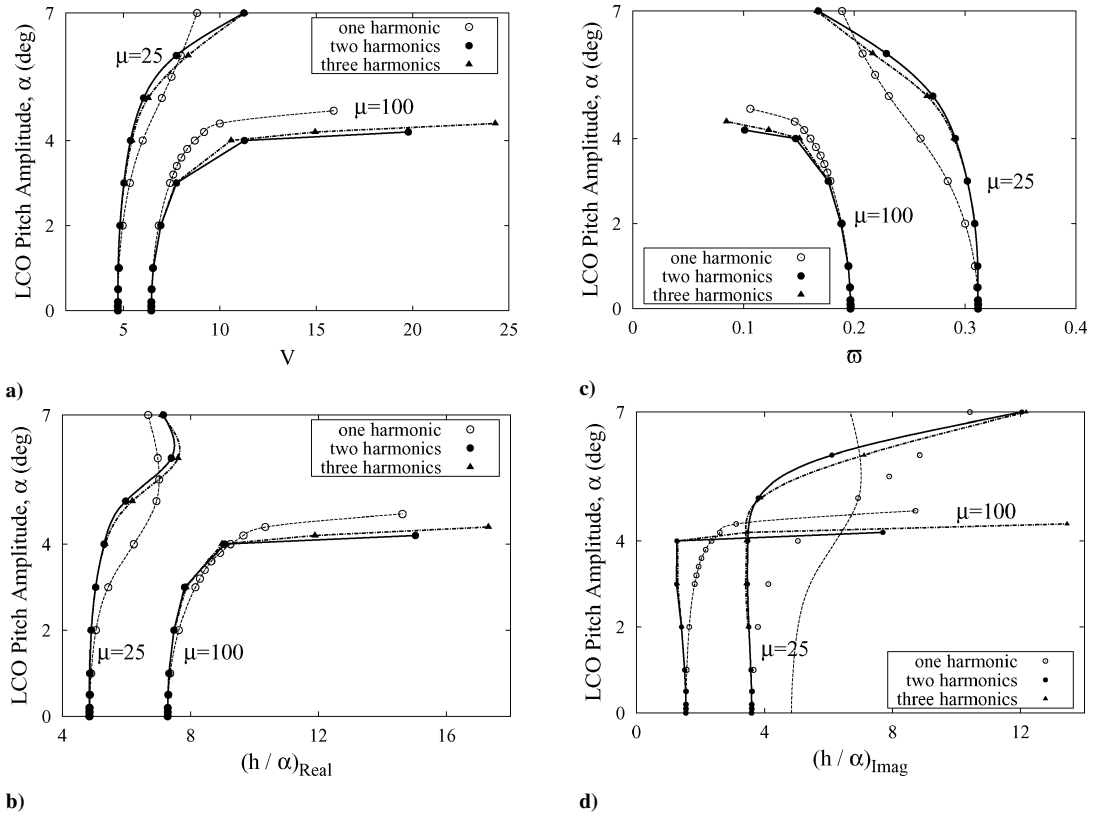

Fig. 2 LCO behavior for $\omega_h/\omega_\alpha = 0.5$ and $M = 0.8$: a) LCO reduced velocity, b) real part of LCO (aeroelastic) eigenvector, c) LCO reduced frequency, and d) imaginary part of LCO (aeroelastic) eigenvector.

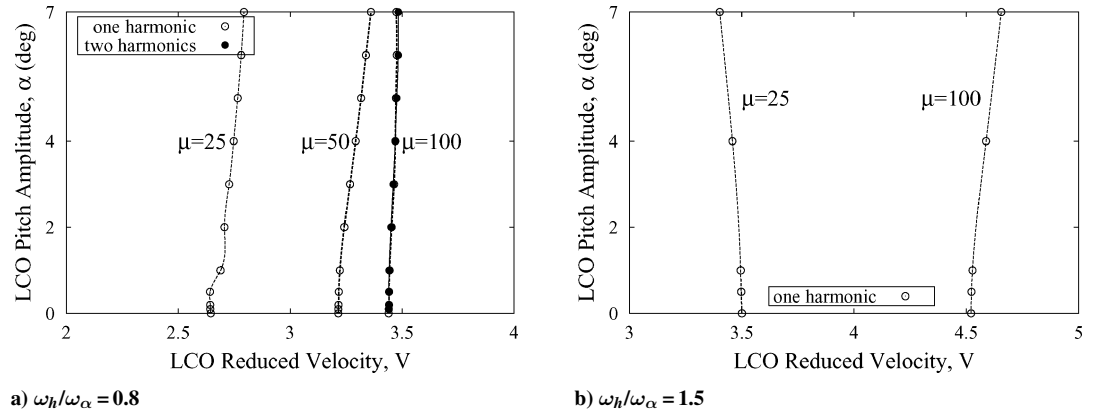

Fig. 3 LCO behavior for $\omega_h/\omega_\alpha = 0.8$, 0.5, and $M = 0.8$.

Figure 3 shows LCO results for frequency ratios of $\omega_h/\omega_\alpha = 0.8$ and 1.5. In both cases the nonlinearity is rather weak—the LCO results depend weakly on the amplitude, that is, the LCO graphs are close to being straight vertical lines.

The present HB/CFD solver has some numerical stability problems for large reduced frequencies, which in turn means that using multiple harmonics for some cases might not work. For the case of $\omega_h/\omega_\alpha = 0.8$ and $\omega_h/\omega_\alpha = 1.5$, the LCO reduced frequency is quite high ($0.5 \leq \bar{\omega} \leq 0.7$), and thus only one harmonic could be used in most instances in the HB solver. However, the authors believe, and the case of $\mu = 100$ in Fig. 3a (where two harmonics were also used) supports this, that when the nonlinearity is weak one harmonic used in the computations of aerodynamic lift and moment can give a reliable LCO result.

There is a difference in the amplitude of the eigenvector (not shown here) for these two frequencies: for $\omega_h/\omega_\alpha = 0.8$, $|\bar{h}/\bar{\alpha}|$ is of the order of one—the motion is a complex pitch–plunge motion, whereas for $\omega_h/\omega_\alpha = 1.5$ it is predominantly pitch motion.

$$\omega_h/\omega_\alpha = 1.8$$

For this rather high frequency ratio (see Fig. 4), the LCO is unstable (for this Mach number at least), especially for the higher mass ratio. The aeroelastic LCO eigenmodes are very much pitch dominated as might be expected. Thus it can be concluded that an increase in the ratio of uncoupled frequency ratio (from $\omega_h/\omega_\alpha = 0.5$ to $\omega_h/\omega_\alpha = 1.8$) is accompanied by changes in stability of the LCO (from stable through weak to unstable) and in the aeroelastic eigenmode (from plunge dominance through pitch–plunge complex motion to pitch dominance). One can also conclude that a higher mass ratio gives rise to a larger nonlinear effect for LCO at this Mach number.

Mach-Number Effects

LCO behavior as a function of Mach number is next studied for two ratios of uncoupled frequencies, $\omega_h/\omega_\alpha = 0.5$ and 0.8 for a mass ratio of $\mu = 100$ (Figs. 5 and 6). Reduced velocity and reduced frequency vs Mach-number trends are shown for various LCO amplitudes including the flutter boundary corresponding to an LCO amplitude of zero. These results allow one to observe the stability of

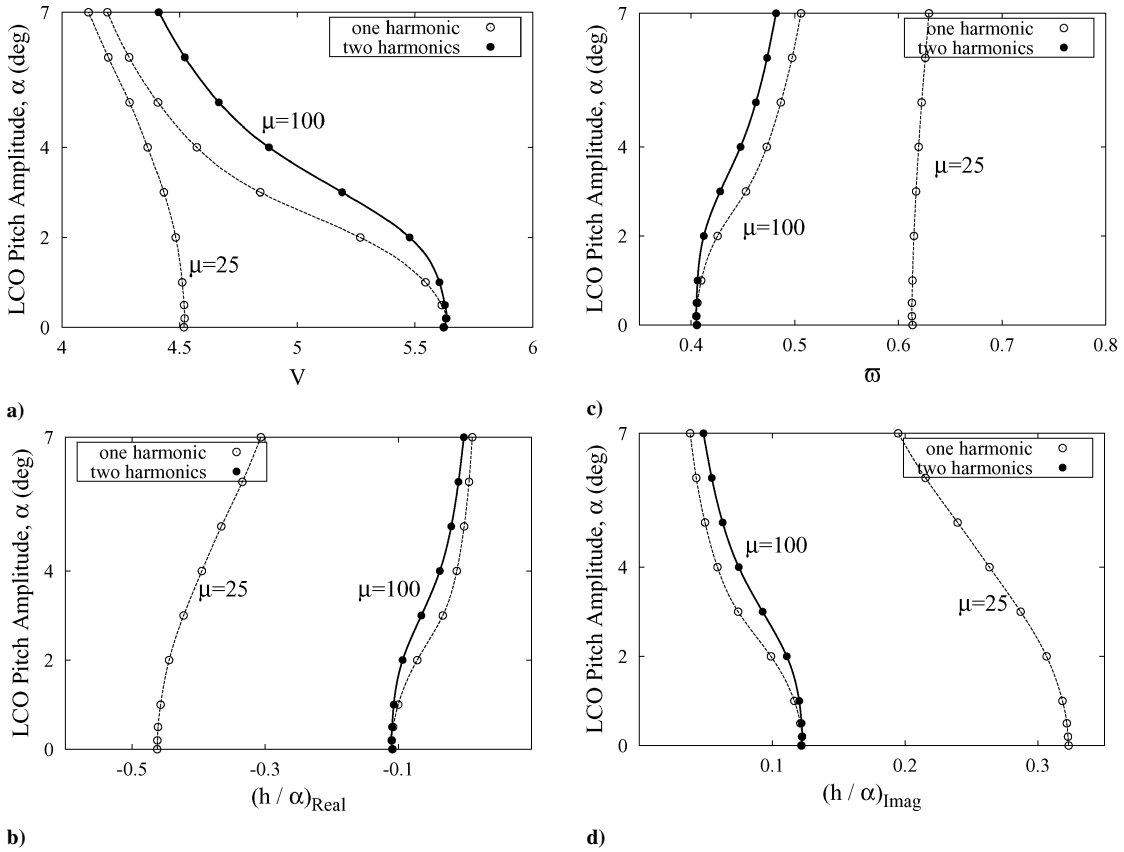

Fig. 4 LCO behavior for $\omega_h/\omega_\alpha = 1.8$ and $M = 0.8$: a) LCO reduced velocity, b) real part of LCO (aeroelastic) eigenvector, c) LCO reduced frequency, and d) imaginary part of LCO (aeroelastic) eigenvector.

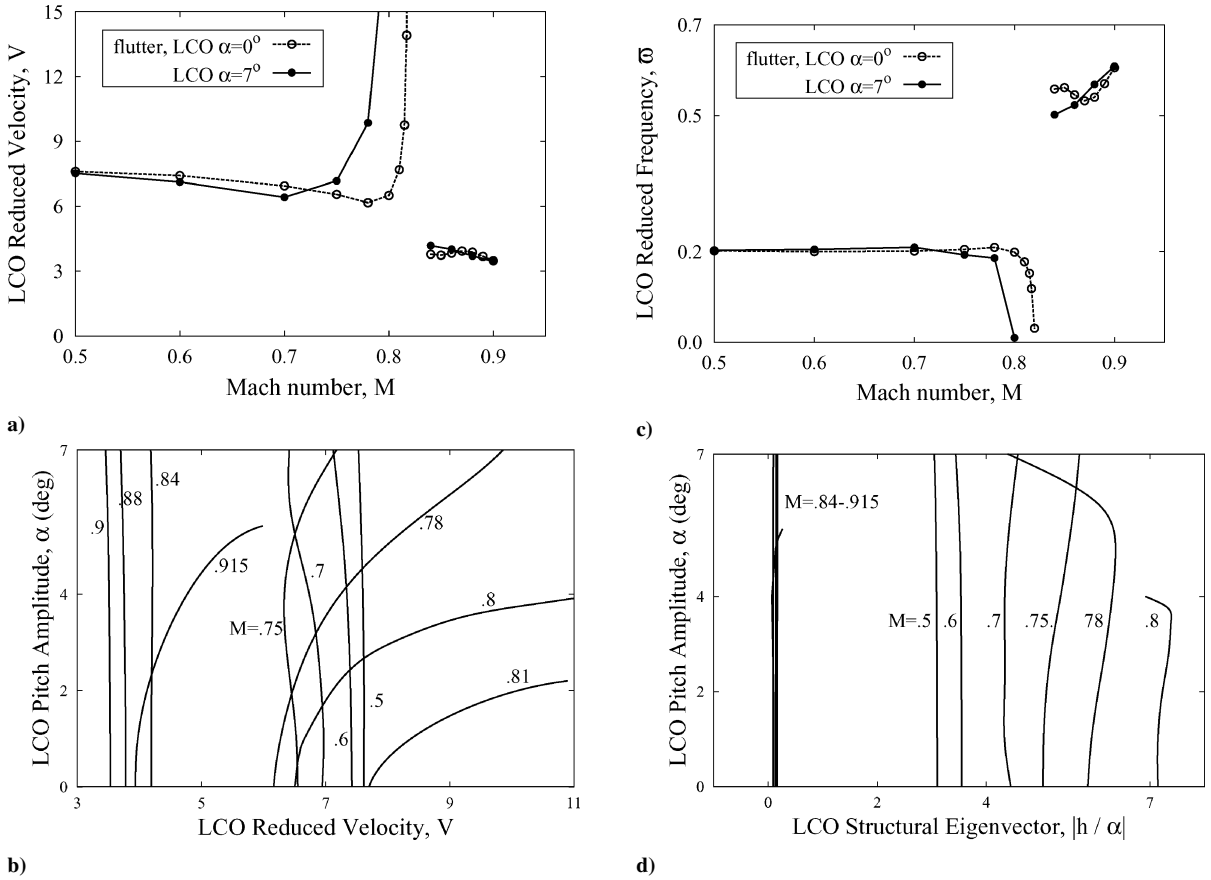

Fig. 5 LCO behavior with respect to Mach number for $\omega_h/\omega_\alpha = 0.5$ and $\mu = 100$: a) LCO reduced velocity vs M, b) LCO amplitude, c) LCO reduced frequency vs M, and d) amplitude of LCO (aeroelastic) eigenvector.

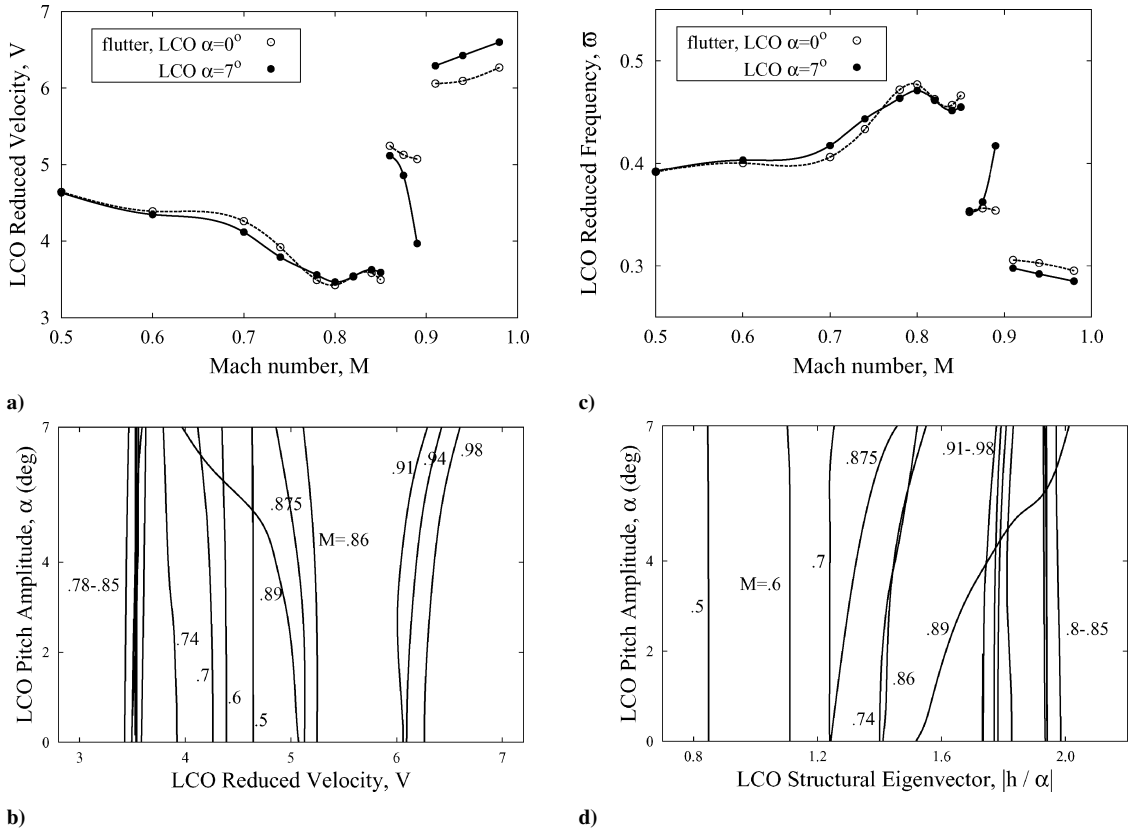

Fig. 6 LCO behavior with respect to Mach number for $\omega_h/\omega_\alpha = 0.8$ and $\mu = 100$: a) LCO reduced velocity vs M, b) LCO amplitude, c) LCO reduced frequency vs M, and d) amplitude of LCO (aeroelastic) eigenvector.

the LCO over a wide range of Mach numbers. Recall that when the LCO reduced velocity is above the flutter reduced velocity the LCO is stable, and when it is below the LCO is unstable. LCO behavior for two frequency ratios are now presented:

$$\omega_h/\omega_\alpha = 0.5$$

The LCO velocity vs Mach-number results in Figs. 5a and 5b show that in the range of $0.78 < M < 0.81$ the aerodynamic nonlinearity effects are strong. In the subsonic Mach-number range $0.5 < M < 0.7$ the LCO is unstable, but only weakly so, with the motion being plunge dominated (see the LCO eigenvectors in Fig. 5d). For $0.75 < M < 0.81$ the LCO becomes strongly stable with predominantly plunge-type motion. Finally, for $0.84 < M < 0.9$ the nonlinearity is very weak, and the motion is pitch dominated.

$$\omega_h/\omega_\alpha = 0.8$$

For this ratio of uncoupled frequencies (Fig. 6), there is also only a small range of Mach numbers where aerodynamic nonlinearity is relatively significant. However, it is interesting to note the numerous changes in the stability of the LCO over the range of Mach numbers considered. LCO are unstable for $0.5 < M < 0.74$, stable for $0.78 < M < 0.85$, unstable again for $0.86 < M < 0.89$, and finally stable again for $0.91 < M < 0.98$. It is not very surprising because of the weak LCO that the LCO eigenvectors are little different from the flutter eigenvectors.[3] The results in Fig. 6d show that the motion is a complex pitch–plunge motion just as was concluded from the flutter results for the corresponding case.[3]

Simulation of a Wind-Tunnel Experiment for Flutter and LCO

Reference 5 provides detailed flutter data from a NACA 0012 Benchmark Model wind-tunnel experiment performed in the NASA Langley Transonic Dynamics Tunnel. In the authors' recent paper[4] a three-parameter flutter surface was obtained for this model (see Fig. 7a). The flutter trajectory (for the values of the speed of sound from Ref. 5) is marked on the computed flutter surface and is compared with those from the wind-tunnel test in Fig. 7b. Typical LCO are shown in Figs. 7c and 7d. These LCO originate from the flutter points A, B, and C that are marked on Figs. 7a and 7b.

It was concluded in Ref. 4 that for a comparison of theoretical results with wind-tunnel flutter data it is advantageous to consider $1/\mu_f$, which is proportional to the air density, as the key parameter. In this case $1/\mu_f$ replaces V in the vector of unknowns, Eq. (3), and the value of the reduced velocity V is kept constant in Eq. (4) and is related to the Mach number through a compatibility relation for a wind tunnel held at constant stagnation temperature. LCO amplitude curves vs $1/\mu_f$ for Mach numbers $M = 0.70$, 0.80, and 0.95 are shown in Fig. 7c. Corresponding LCO amplitude vs V results for constant $\mu \approx 4000$, 5200, and 2700 respectively are shown in Fig. 7d. These three cases are good examples of 1) A, weakly unstable LCO (in terms of LCO amplitude vs inverse mass ratio or reduced velocity) that become stable at higher amplitudes ($M = 0.70$); 2) B, strong stable LCO that become unstable ($M = 0.80$); and 3) C, weak LCO ($M = 0.95$). The similarity of Fig. 7c to Fig. 7d suggests that the key parameter at these Mach numbers is dynamic pressure rather than mass ratio or flutter velocity per se.

Note however that the flutter boundary drops precipitously in Fig. 7b for a certain Mach-number range, that is, $0.82 < M < 0.92$. This is because of the change in flutter mode to single-degree-of-freedom flutter caused by negative aerodynamic damping. At realistic mass ratios $1/\mu > 0.0001$, it appears the LCO amplitudes are very large, although this can be modified if structural damping were included in the aeroelastic modes.

For earlier studies of the LCO of a typical section airfoil, please see the paper by Thomas et al.[2] There preliminary results were shown establishing the feasibility of the present approach.

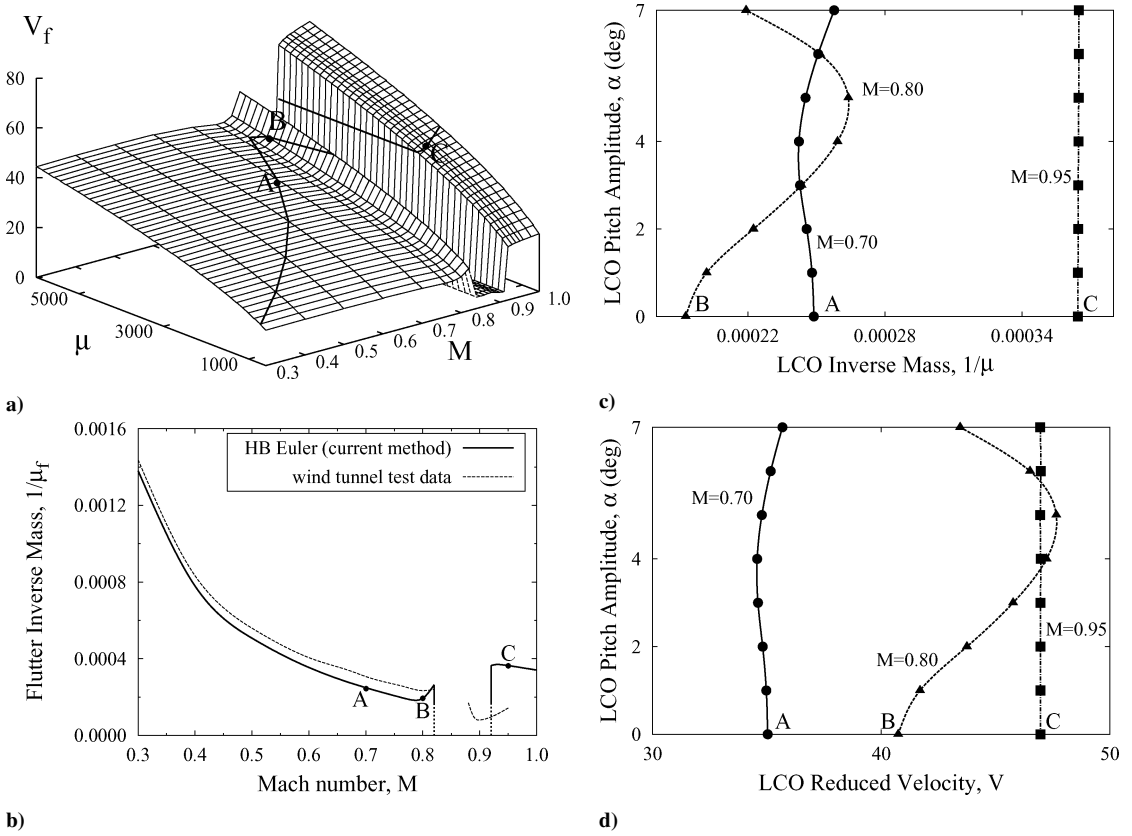

Fig. 7 Numerically simulated wind-tunnel flutter trajectory and LCO. (NACA 0012, $\omega_h/\omega_\alpha = 0.646$, $x_\alpha = 0$, $r_\alpha^2 = 1.024$, and $a = 0.$): a) three-parameter flutter surface with the numerically simulated wind-tunnel trajectory as indicated, b) comparison of computational flutter results with those from winde-tunnel testing, c) LCO amplitude vs inverse mass, and d) LCO amplitude vs reduced velocity.

Conclusions

Using a state-of-the-art Euler computational-fluid-dynamics-based aerodynamic code, an investigation is presented of how structural and aerodynamic parameters (including freestream transonic Mach number) affect limit-cycle-oscillation (LCO) characteristics of a typical two-degree-of-freedom airfoil configuration. The following conclusions have been drawn.

A study of the effect of the ratio of uncoupled natural frequencies ω_h/ω_α determined that the reduced velocities have a minimum near $\omega_h/\omega_\alpha \approx 1$ for a given LCO amplitude. For the considered Mach number $M = 0.8$ when the ratio of uncoupled natural frequencies is well below 1, the LCO is found to be stable, and when this ratio is well above one, the LCO is found to be unstable.

It is also demonstrated that the LCO solutions are very sensitive to Mach number especially in the transonic range. Depending on the frequency and the mass ratios, there might (or might not) be sudden and significant changes in the type of LCO motion as the Mach number is varied. Moreover, it is found that the aerodynamic nonlinearity is most prominent in a limited range of transonic Mach numbers and rather weak outside this Mach-number range. Finally, the stability of LCO is also found to change abruptly with respect to Mach number.

In summary a parametric aeroelastic analysis of an airfoil configuration has been conducted using a highly efficient harmonic-balance computational technique. Computational results agreed well with a wind-tunnel flutter test, although correlation with experimental LCO results remains an open challenge. The theoretical LCO results presented here might provide an impetus for future LCO experiments.

References

[1]Hall, K. C., Thomas, J. P., and Clark, W. S., "Computation of Unsteady Nonlinear Flows in Cascades Using a Harmonic Balance Technique," *AIAA Journal*, Vol. 40, No. 5, 2002, pp. 879–886.

[2]Thomas, J. P., Dowell, E. H., and Hall, K. C., "Nonlinear Inviscid Aerodynamic Effects on Transonic Divergence, Flutter and Limit Cycle Oscillations," *AIAA Journal*, Vol. 40, No. 4, 2002, pp. 638–646.

[3]Kholodar, D. B., Thomas, J. P., Dowell, E. H., and Hall, K. C., "A Parametric Study for an Airfoil in Inviscid Transonic Flow," *Journal of Aircraft*, Vol. 40, No. 2, 2003, pp. 303–313.

[4]Kholodar, D. B., Dowell, E. H., Thomas, J. P., and Hall, K. C., "Improved Understanding of Transonic Flutter: A Three Parameter Flutter Surface," *Journal of Aircraft*, Vol. 41, No. 4, 2004, pp. 911–917.

[5]Rivera, J. A., Dansberry, B. E., Bennett, R. M., Durham, M. H., and Silva, W. A., "NACA 0012 Benchmark Model Experimental Flutter Results with Unsteady Pressure Distributions," NASA TM 107581, March 1992.